published in Proc. SPIE 4838, 668–679, 2003

Design of spatial and modal filters for nulling interferometers

Oswald Wallner[a], Walter R. Leeb[a] and Reinhold Flatscher[b]

[a] Vienna University of Technology, Austria
[b] Astrium GmbH, Friedrichshafen, Germany

ABSTRACT

Spatial or modal filters are essential parts of highly rejecting nulling interferometers. We review the principle of operation of both types of filters and explain the fundamental physical difference. We point out the filter's individual properties and potentials, and analyze practical limitations. For modal filters we discuss implementation alternatives, also with regard to their suitability for mid-infrared operation. For a single-mode fibre filter we analyze the broadband performance and the minimum length ensuring a prescribed filter action. We further present simulation results of a DARWIN-representative nulling interferometer breadboard which confirm the distinct improvement in rejection ratio due to spatial or modal filtering.

Keywords: nulling, interferometry, spatial filter, modal filter, single-mode waveguide, pinhole

1. NULLING INTERFEROMETRY

Both the European DARWIN[1] mission and the United States TPF[2] project are eyed on investigating Earth-like exoplanets orbiting Sun-like stars at an interstellar distance up to 25 parsecs. The requirements on instruments dedicated to visual detection and imaging of such planets are challenging due to the small angular separation of about 40 mas and the large contrast ratio which, even in the mid-infrared, amounts to some 10^6. Further challenges are caused by the large bandwidth of 4 to 20 microns, determined by the scientific goal of spectroscopically observing absorption lines of biomarkers.

A nulling interferometer, as proposed by Bracewell[3] in 1978, provides both high on-axis light suppression due to a strong dependence of the transmission on the light's angle of incidence and high angular resolution due to a large baseline. In the simplest arrangement, the sum of star and planet waves is received by two identical telescopes. One of the resulting signals is subject to a phase change of π and both signals are superimposed to obtain interference. The star light is strongly reduced by the (quadratic) on-axis null of the interferometer's transmission map, while the planet's light experiences constructive interference by proper adjustment of the baseline.

The rejection ratio R of such a nulling interferometer, defined as the interferometer's output power at constructive interference to that at destructive interference, i.e. $R = P_c/P_d$, is strongly influenced by wavefront errors induced by environmental or instrumental disturbances. As shown in Tab. 1, the requirements[4] on uniformity of phase, amplitude, and state of polarization among the two interferometer arms are stringent. Obviously, some of these requirements can hardly be met in practice. However, especially the application of modal filters makes highly rejecting nulling interferometers feasible: Such filters may eliminate the effect of local disturbances within the amplitude profile and the phasefront.

Send correspondence to:
Oswald Wallner,
Institute of Communications and Radio-Frequency Engineering,
Gusshausstrasse 25/389, 1040 Vienna, Austria (Europe),
E-mail: oswald.wallner@ieee.org,
Telephone: ++43-1-58801-38996

error source		requirement to achieve a given rejection ratio R at the wavelength λ	
		general	$R = 10^6$ at $\lambda = 10\mu m$
local defect	rms pointing error	$8\lambda/(\pi D\sqrt{R})$	$2.5 \cdot 10^{-8} m/D\ rad$
	rms phase fluctuations*	—	$2.3\,nrad$
	rms amplitude fluctuations*	—	$2 \cdot 10^{-3}$
global defect	optical path delay error	$\lambda/(\pi\sqrt{R})$	$3.2\,nm$
	relative intensity error	$2/\sqrt{R}$	0.2%
	differential change of polarization	$2/\sqrt[4]{R}$	$63\,mrad$
	differential birefringence	$\lambda\sqrt{2/R}/\pi$	$4.5\,nm$

Table 1. Requirements on phase, amplitude, and polarization of the beams in a two-arm nulling interferometer (D denotes the telescope diameter, the symbol $*$ indicates numerically obtained results).

2. SPATIAL AND MODAL FILTERING

When speaking about "spatial" filtering, one should distinguish between truly spatial filtering and modal filtering. These concepts are based on completely different physical principles. Spatial filtering means blocking of certain spatial frequencies, analogous to frequency filtering in electronics. Modal filtering means the projection onto a field with predefined amplitude and phase distribution.

2.1. Spatial filtering

Spatial filtering[5,6] is based on blocking spatial frequencies exceeding a certain spatial frequency. This can be realized by a setup as shown in the upper part of Fig. 1. The incoming field E_{in} is laterally confined by a circular aperture of radius a and focussed by a lens of focal length f onto a pinhole of radius b, located in the lens' back focal plane. As the field transformation performed by the lens is given – in a paraxial approximation – by $\mathcal{F}\{\cdot\}/(\lambda f)$, where $\mathcal{F}$ is the Fourier operator and λ is the wavelength, the field in the focal plane, E_{foc}, is the spatial frequency representation of the apertured input field, i.e. $E_{\text{foc}}(r) = E_{\text{foc}}(\nu_r) = \mathcal{F}\{E_{in} \cdot A\}/(\lambda f)$, where r is the radial coordinate, A is the aperture function and $\nu_r = r/(\lambda f)$ is the spatial frequency (unit m^{-1}). The pinhole of radius b therefore blocks all spatial frequencies larger than $\nu_r > b/(\lambda f)$. Thus a setup as given in Fig. 1 works as a spatial low-pass filter.

The potential rejecting high spatial frequency defects is illustrated in the lower part of Fig. 1. A plane input field with a small-scale distortion is focussed onto the pinhole. Because of the linearity of the Fourier operator, we can treat the plane field and the distortion separately. The plane field is transformed into an Airy pattern with a central lobe of width $1.22\,\lambda f/a$. If the pinhole diameter b is chosen properly, the central portion of the Airy pattern will pass. The distortion results in an Airy pattern as well, but, because of the small size of the defect, it is much broader. As only the small central part can pass the pinhole, the contribution of the defect to the total field is drastically reduced. The dotted lines indicate that parts of the field distributions which are blocked by the pinhole.

The choice of the pinhole radius is basically determined by the lens, characterized by the focal length f and the pupil radius a, and by the wavelength λ. However, the actual value is given by a trade-off between the filter's insertion loss and the filter bandwidth. If we demand that the central Airy lobe of a plane field should pass, the pinhole radius has to equal the Airy radius, i.e. $b = r_s = 1.22\,\lambda f/(2a)$. This results in a spatial filter bandwidth of $\nu = 0.61/a$ and in an insertion loss of 16%.

Spatial filters realized by pinholes have the advantage of being very simple. However, they are not suitable for high-contrast nulling interferometry because of the following drawbacks:

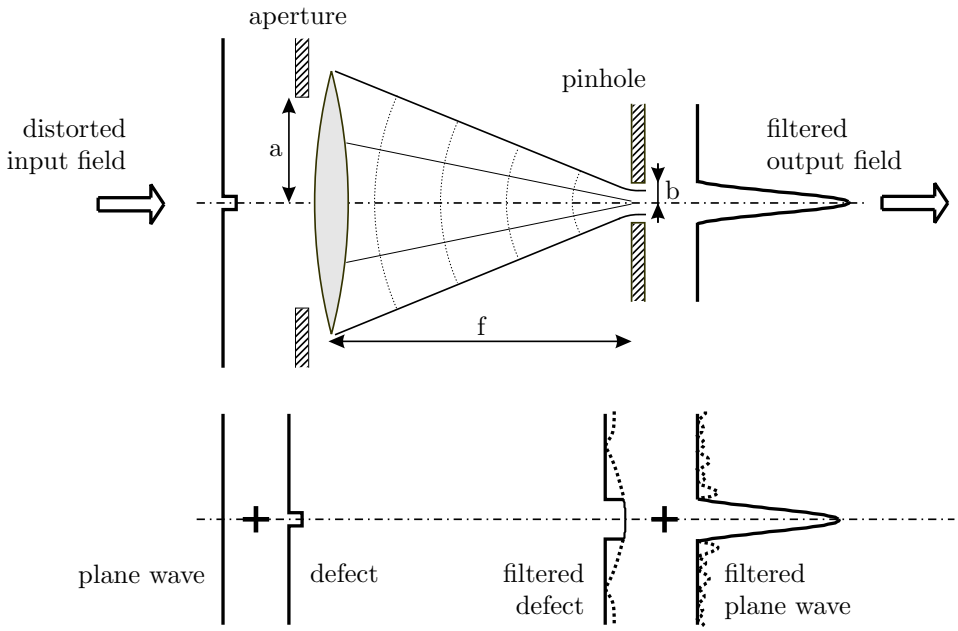

Figure 1. Fundamental layout and principle of operation of a spatial filter realized by a pinhole.

- Because of the low-pass characteristic of the pinhole, amplitude and phase distortions with spatial frequencies smaller than the bandwidth $b/(\lambda f)$ are not eliminated but pass the filter.
- Pinholes are highly chromatic concerning filter bandwidth and optical throughput. For a given setup (lens and pinhole) the filter bandwidth reduces with increasing wavelength. This goes hand in hand with better filtering, but at the cost of insertion loss. In the limit of an infinitely small pinhole diameter the wavefront filtering is perfect but the optical throughput is zero.

2.2. Modal filtering

A modal filter[4, 7] is an optical element which provides at its output a field with unique amplitude and phase distribution, irrespective of the input field. Single-mode waveguides show this behavior, at least in principle. The input field is projected onto the waveguide's orthonomal eigenmodes F_i, i.e. the field is represented as $\sum_i a_i F_i$, where the a_i are the modal amplitudes. If, by proper choice of wavelength, refractive indices, and waveguide geometry, only one mode can propagate ($a_i = 0$ for $i \neq 0$), the waveguide acts as a modal filter.

The principle setup of a modal filter is shown in the upper part of Fig. 2. The input field E_{in} is focussed onto the waveguide's input face by a lens of focal length f and free radius a, resulting in the field E_{foc}. In general, an infinite number of modes are excited. However, all modes but the waveguide's fundamental mode are radiated off, thus leading to a spatial steady state after a certain distance where only the fundamental mode is present in the vicinity of the fibre axis.

The filter's output field is characterized by a plane phasefront and an amplitude profile which is solely determined by the waveguide's physical properties. For an ideal waveguide, the output field is proportional to the waveguide's fundamental mode F_0, i.e. $E_{\text{out}} = \zeta \cdot F_0$, where F_0 is normalized to an overall power of unity. The peak amplitude and phase shift are determined by the complex field coupling efficiency ζ between the waveguide's input field E_{foc} and the fundamental mode, i.e. by

$$\zeta = \iint_A E_{\text{foc}}\, F_0^*\, dA \quad . \tag{1}$$

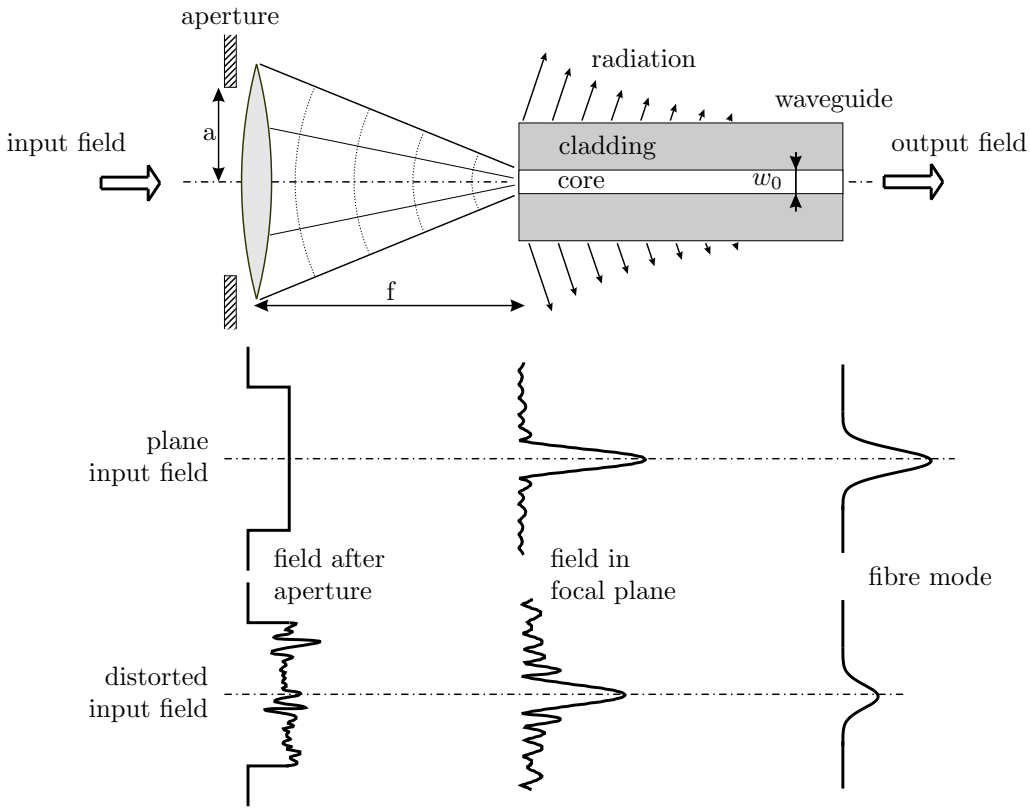

Figure 2. Fundamental layout and principle of operation of a modal filter realized by a single-mode step-index fibre.

With F_0^* we denote the complex conjugate of eigenmode F_0, A is the coupling area. For an ideal waveguide which provides only its fundamental mode at the output, the coupling efficiency ζ is the quantity which determines the filter action and the insertion loss of a modal filter.

As it can be seen in the lower part of Fig. 2, irrespective of the input field the output field always equals the waveguide's fundamental mode. Of course, input wave phasefront and amplitude profile perturbations cause a reduction of the overall output power (squared modulus of ζ) and a slight additional phase shift (phase of ζ).

Broadband operation

When designing modal filters for the application in mind one has to ensure single-mode operation over the whole wavelength range in question. Optimum performance can only be achieved at one wavelength, the design wavelength λ_0. For fixed lens and waveguide parameters, the coupling efficiency and therefore also the filter action changes significantly with changing wavelength. Figure 3 shows the coupling efficiency dispersion for the case of coupling a plane wave to a single-mode fibre. The solid lines present the coupling efficiency dispersion for the case where the coupling system (lens and fibre) is optimized for maximum coupling at the specified normalized frequency V_{opt}. The theoretically maximum value of $|\zeta|^2 = 0.786$ is achieved for a system with a normalized frequency $V = 2\pi\rho/\lambda(n_{\mathrm{co}}^2 - n_{\mathrm{cl}}^2)^{1/2}$ equal the single-mode cutoff frequency $V_c = 2.405$, where ρ is the core radius and n_{co} and n_{cl} are the core and cladding refractive indices ($\eta = |\zeta|^2$ is known as power coupling efficiency[8]). For calculating ζ not an approximation but the exact field was used for the fibre's fundamental mode. For lower values of V, less maximum power can be coupled into the fundamental mode because the overlapping between the fibre's input field and the fundamental mode reduces. The coupling efficiency drops to almost zero within two octaves. This prevents broadband operation as almost all power is lost at the upper end of the wavelength range. However, appropriate filter action is possible anyway. If the lens' f-number is

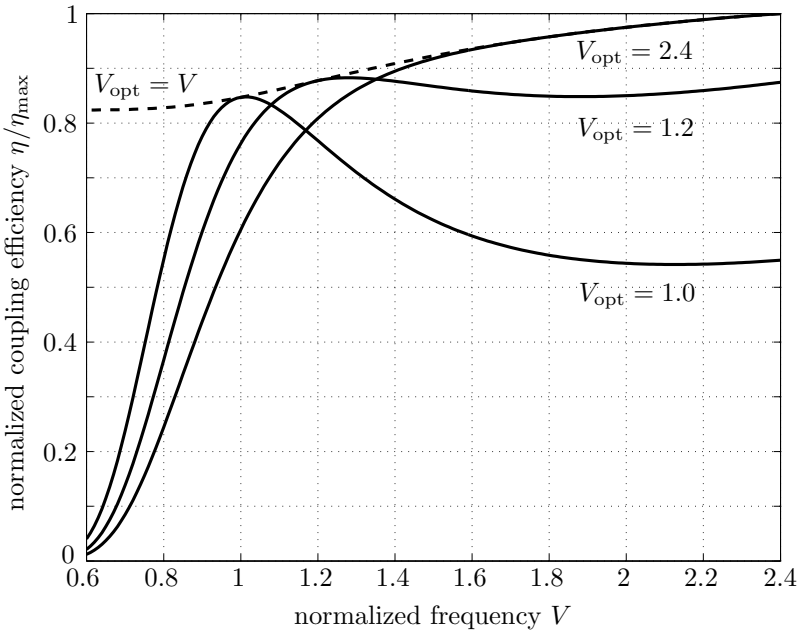

Figure 3. Coupling efficiency dispersion.

optimized for maximum coupling for each value of V, i.e. $V_{\text{opt}} = V$, only 20% of coupling efficiency are lost within two octaves (broken line). This would be relevant for a system where the desired wavelength range is split into several bands.

Minimum filter length

The optical field incident onto the waveguide's input face excites, in general, an infinite number of modes. All modes but the waveguide's fundamental mode are radiated off, thus leading to a spatial steady state after a certain distance where only the fundamental mode is present. To achieve a specified degree of filter action, a certain minimum waveguide length z_0 is required. For two reasons one should aim to make waveguides dedicated to modal filtering as short as possible. Firstly, materials transmitting in the mid-infrared are absorbing, thus longer filters will show increasing insertion loss. Secondly, the longer the fibre the larger the possibility to induce unwanted effects during the fabrication process (e.g. scattering centers) or during operation (e.g. bending).

To make a worst-case estimate of the minimum length of an ideal step-index fibre filter we calculated the attenuation of that leaky mode which suffers lowest attenuation.[9] We define the filter action as the ratio of the fundamental mode power to the power in this leaky mode, i.e. $A = P_{F_0}/P_{LM}$. The minimum length is determined by

$$\frac{z_0}{\rho} = \frac{1}{\alpha\rho}\ln\frac{A(1-\eta)}{\eta} \quad , \tag{2}$$

where ρ is the core radius, α is the leaky mode's attenuation factor, and η is the power coupling efficiency.

Figure 4 shows the minimum filter length z_0 as a function of wavelength λ for three different core diameters 2ρ. For this calculation we assumed an attenuation factor of $A = 10^6$ (corresponding to the actual requirements for the interferometers DARWIN and TPF) and typical parameters of a silver halide fibre, i.e. $n_{co} = 2.18$ and $\Delta = 0.25\%$. The solid lines give the case of good coupling, i.e. $\eta = 0.78$ at single-mode cutoff, and the broken lines the case of poor coupling with $\eta = 0.1$.

Minimum cladding diameter

If a single-mode fibre is used as a broadband high-quality spatial filter, it has to be guaranteed that the cladding diameter is sufficiently large in order to minimize the effect of the cladding/air interface on the guided mode.

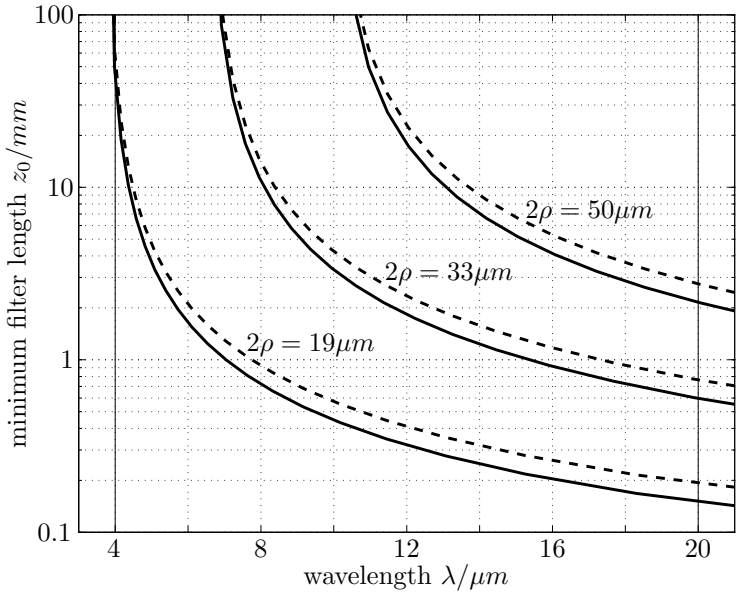

Figure 4. Minimum filter length z_0 as a function of wavelength λ for typical parameters of silver halide fibres, i.e. $n_{co} = 2.18$, $\Delta = 0.25\%$, and core diameters $2\rho = 19\mu m, 33\mu m$ and $50\mu m$. The attenuation factor is $A = 10^6$. The solid lines give the case of $\eta = 0.78$ at single-mode cutoff, the broken lines the case of $\eta = 0.1$.

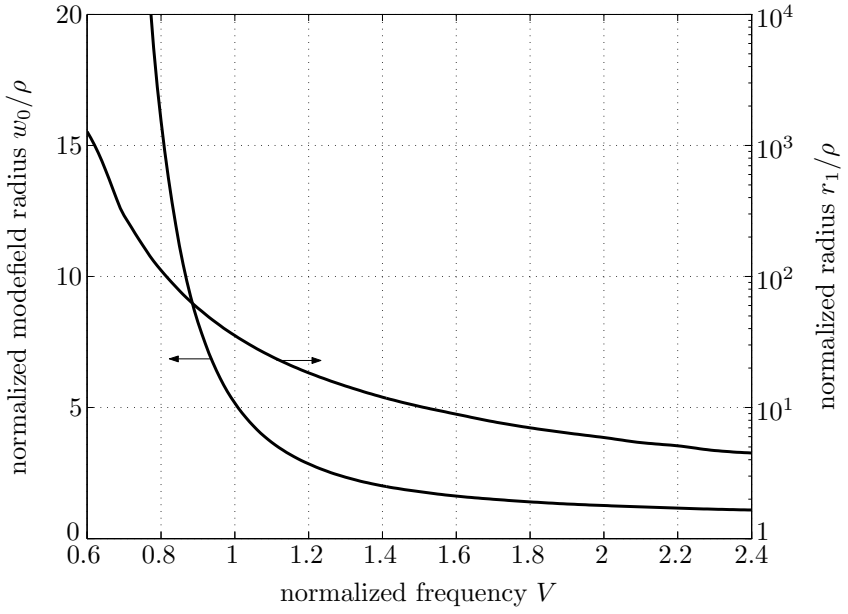

Figure 5. Modefield radius dispersion and cladding diameter dispersion.

Figure 5 shows the modefield radius dispersion of a single-mode fibre. We define the modefield radius w_0 as that $1/e$-radius of a Gaussian distribution which ensures maximum coupling with the fibre mode. Close to single-mode cutoff the modefield radius is only slightly larger than the core radius. However, two octaves below cutoff it enlarges dramatically. The second curve in Fig. 5 shows that radius r_1 outside which the residual power amounts to 10^{-6} of the total guided power. This radius can be interpreted as the required cladding radius to ensure negligible influence of the cladding boundary.

3. MODAL FILTERS FOR THE MID-INFRARED

Any optical waveguide which can be designed to be single-mode within a certain bandwidth is, in principle, suitable for modal filtering. Because of technological difficulties in realizing the lateral waveguide geometry and because of difficulties with processing mid-infrared materials, not all of these waveguide structures can be manufactured today.

3.1. Filter geometries

Examples of optical waveguides which can be designed to support only one mode within a certain bandwidth are shown in Fig. 6. Note that hollow fibres, i.e. cylindrical structures with an air core and a cladding made of some reflecting material, are inherently multi-mode and therefore not suitable for high-accuracy spatial filtering.

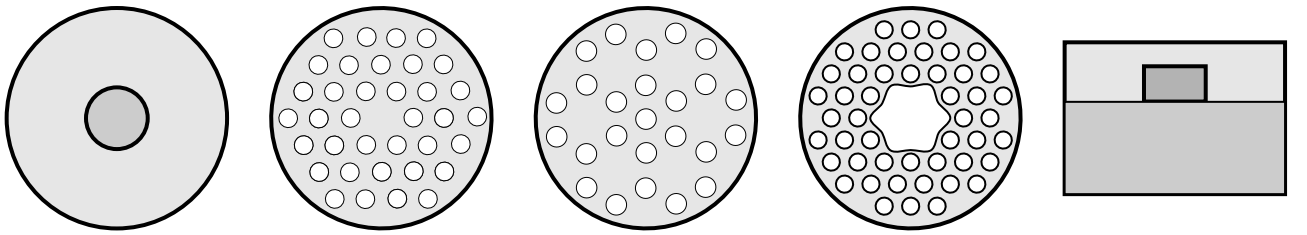

Figure 6. Optical waveguides which allow for single-mode operation.

1. Step-index fibre
A step-index fibre, i.e. a cylindrical rod of refractive index n_{co} surrounded by a cladding material of lower refractive index $n_{cl} < n_{co}$, performs waveguidance by compensating the diffraction spreading by reducing the local phase velocity at the beam center.[10] The range of possible values for the propagation constant β is therefore given by $k\,n_{cl} < \beta < k\,n_{co}$, with $k = 2\pi/\lambda$. For normalized frequencies $V < V_c = 2.405$, corresponding to wavelengths $\lambda > \lambda_{min} = 2.61\rho(n_{co}^2 - n_{cl}^2)^{1/2}$, such fibres support only a single mode, the fibre's fundamental mode LP_{01}. Because the fundamental mode has a cutoff frequency of zero, optical fibres have an infinitely large single-mode bandwidth.

Fibres with a power-law refractive index profile have similar properties as step-index fibres. Such refractive index profiles are appropriate to model the smoothed-out profiles resulting form actual fibre manufacturing processes. The single-mode cutoff frequency V_c is a function of the power-law exponent g and approximately[11] given by $V_c = 2.405 \cdot (1 + 2/g)^{1/2}$.

2. Index-guiding photonic crystal fibres
An index-guiding photonic crystal fibre (PCF) is formed by a (not necessarily) periodic structure of air holes at wavelength scale, embedded in some dielectric material. A defect which confines the light and therefore acts as core is introduced by omitting one air hole. Waveguidance can be explained by considering that the cladding region provides an effective index[12] n_{eff}. Because n_{eff} is smaller than the core index, i.e. the index n_m of the dielectric material, light is guided by the same effect as in conventional fibres, despite the complicated structure. The range of possible values for the propagation constant β is therefore given by $k\,n_{\text{eff}} < \beta < k\,n_m$.

Analogous to conventional fibres, an effective fibre parameter $V = 2\pi\Lambda(n_m^2 - n_{eff}^2)^{1/2}/\lambda$ can be defined, where Λ is the center-to-center hole spacing. In contrast to conventional fibres, V_{eff} approaches a constant value for decreasing λ as the effective cladding index approaches the core index for $\lambda \to 0$. Thus, for sufficiently small relative air hole diameter d/Λ, single-mode operation for all wavelengths λ and hole distances Λ can be obtained.

3. PBG-guiding photonic crystal fibres
Photonic crystals, i.e. structures with – at wavelength scale – periodically varying refractive index, can exhibit photonic bandgaps (PBG). These are frequency intervals where light propagation is forbidden in certain directions. Light with frequencies within a PBG will be completely reflected by Bragg reflection. By locally breaking the periodicity of the crystal via introducing a well-defined defect, e.g. in form of an extra air hole, light can be confined and thus guided, provided that the surrounding photonic crystal cladding exhibits a PBG at the operation frequency.[13] A remarkable difference between PBG-guiding PCFs and conventional fibres or index-guiding PCFs is that there are regions, i.e. photonic bandgaps, below the effective cladding index where guided modes can exist.

The high degree of flexibility makes PBG-guiding PCFs very attractive. The photonic bandgap regions, i.e. the transmission windows, are determined by the cladding structure only. The behavior of the guided modes inside the photonic bandgap is solely determined by the characteristic of the defect. By varying size and shape of the defect, the frequency of the guided mode can be positioned precisely in a photonic bandgap. The drawback is that the transmission windows which can be practically realized are narrow and therefore do not allow for broadband operation.

4. Air-guiding photonic crystal fibres
PBG-guiding PCFs have the drawback that the guided modes extend substantially into the cladding material, which, especially with regard to mid-infrared operation, leads to a high insertion loss. This problem can be overcome by introducing a large air core,[14] provided that the cladding structure exhibits at least one photonic bandgap that covers mode indices $\beta\lambda/(2\pi)$ equal or less than unity (which corresponds to the refractive index of air). The main drawback of this type of fibres is that the leakage-free operational windows are limited to a few tens of nanometers.

5. Integrated optics waveguide
Integrated optics waveguides consist of a rectangular core surrounded by a cladding which is formed by one or more regions of lower refractive index. Similar to fibres, integrated optical waveguides support several guided modes, depending on the wavelength, the core dimensions, and the refractive indices.[15] All these modes have a cutoff value, thus the waveguide can be designed for single-mode operation. Because also the fundamental modes has a finite cutoff wavelength, the single-mode bandwidth is somewhat smaller than that of conventional fibres.

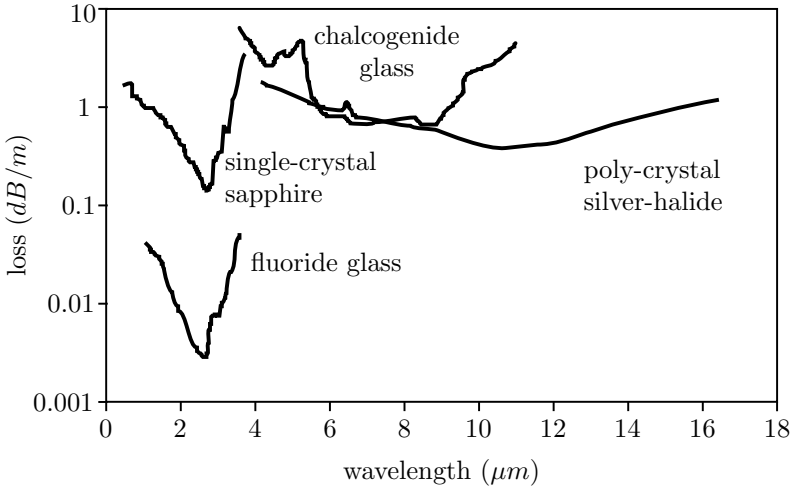

Figure 7. Loss spectra of some mid-infrared materials.[16]

3.2. Dielectric materials

Glassy or crystalline dielectric materials as those named in Fig. 7 are suitable for transmitting mid-infrared radiation. In general, both the optical and mechanical properties of waveguides made from these materials remain inferior to that of silica waveguides. Typical attenuations amount to several dB/m

Chalcogenide glass and poly-crystalline silver-halide seem to be the most suitable materials for developing waveguides to be single-mode in the mid-infrared wavelength range above $4\,\mu m$. Chalcogenide glass has a transmission range form about 4 to $11\,\mu m$ and a typical attenuation of $1\,dB/m$ at $10.6\,\mu m$. Silver-halide is transparent from 3 to $20\,\mu m$ and the loss at $10.6\,\mu m$ can be as low as $0.5\,dB/m$. The manufacturing processes of both types of materials are well developed for multi-mode fibres, but are only in a test-phase for single-mode fibres. The required reduction of the core diameter seems to be easier for glassy materials than for crystalline ones.

4. BREADBOARD SIMULATION

In order to substantiate the performance of a DARWIN interferometer, a breadboard operating in the near-infrared has been established. As schematically shown in Fig. 8, the breadboard consists of a source simulator, achromatic phase shifters, actively controlled optical path delay lines, an interferometer core, spatial or modal filters at the scientific output, and an internal metrology (a detailed description is given by Flatscher[17]). In the following we present breadboard simulation results which confirm the distinct improvement in rejection ratio when employing a modal filter.

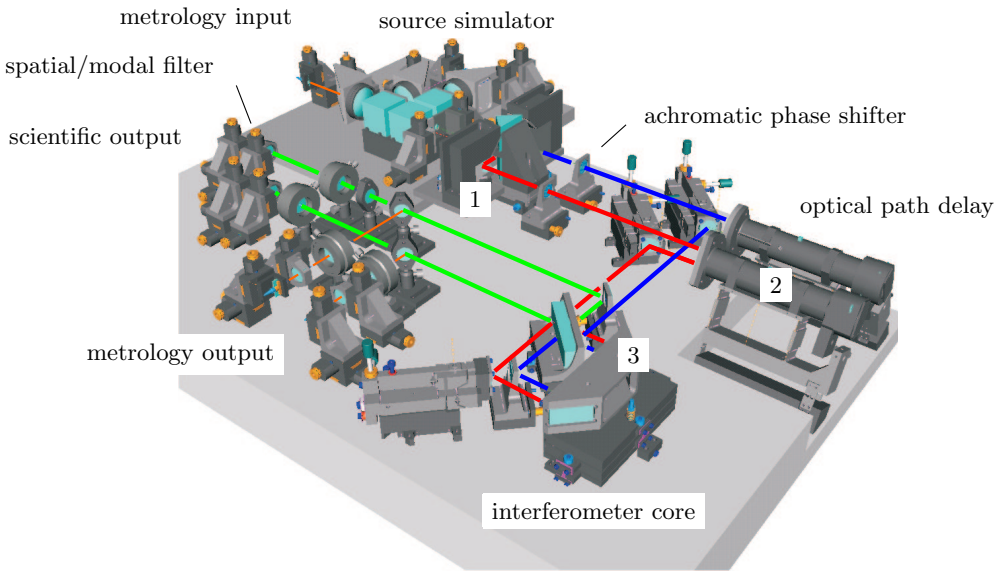

Figure 8. Nulling interferometer breadboard.[17]

Deep nulling with rejection ratios in the order of 10^6 – as it should be demonstrated by the breadboard – requires a high degree of uniformity of the wavefronts to be combined. This can only be attained by a highly symmetric optical setup as it is given for the superimposing part by a fully symmetric Sagnac interferometer core.[18] The source simulator, based either on amplitude or on wavefront division, seriously influences the symmetry. However, appropriate phase shifter concepts, as e.g. a periscope, allow for reestablishing the symmetry. Numerical examples of the nulling capability of a breadboard without any imperfections but with different source concepts and different phase shifter implementations are given in Tab. 2.

- The wavefront dividing source concept leads to asymmetric interferometer input beams and thus, if dispersive phase shifters are used, to sufficient nulling only if a modal filter is employed (case 1). No filter is required in case of a periscope phase shifter as it flips the fields and therefore reestablishes the symmetry (case 2).
- The amplitude dividing source concept is inherently symmetric. Spatial or modal filters therefore do not improve the nulling capability (case 3 and 4). The rejection ratio of case 3 is lower than that of case 4 because the plates are not perfectly optimized for the wavelength used.

case		1	2	3	4
source concept		wavefront division		amplitude division	
phase shifter		dispersive	periscope	dispersive	periscope
rejection ratio	without filtering	$6.8 \cdot 10^1$	$2.5 \cdot 10^9$	$4.2 \cdot 10^7$	$2.5 \cdot 10^9$
	with pinhole	$2.6 \cdot 10^2$			
	with modal filter	$1.4 \cdot 10^6$			

Table 2. Simulation results for different source concepts and phase shifter implementations for a breadboard without any misalignment.

Although a perfectly aligned optical system was assumed for case 1, it illustrates the potential of modal filters for correcting local wavefront defects, which, in this case, are caused by the asymmetric source concept. In Tab. 3 we present three types of misalignment which also cause local wavefront defects, namely transversal and axial shift, and tilt. To be able to identify the effect of each individual imperfection, we assume the symmetric amplitude division source concept.

case		3	5	6	7
source concept		amplitude div.	amplitude division		
phase shifter		dispersive	dispersive		
misalignment		—	*transversal shift* of mirror feeding the delay line: $0.1\,mm$	*defocus* of delay line's flat secondary mirror: $4.1\,\mu m$	*tilt* of mirror within interferometer core: $1\,arcsec$
control		—	optical path delay control		
rejection ratio	without filtering	$4.2 \cdot 10^7$	$1.8 \cdot 10^3$	$3.2 \cdot 10^2$	$8.1 \cdot 10^1$
	with pinhole		$1.3 \cdot 10^4$	$1.3 \cdot 10^3$	$3.3 \cdot 10^2$
	with modal filter		$4.1 \cdot 10^7$	$3.4 \cdot 10^4$	$1.2 \cdot 10^6$

Table 3. Simulation results for different types of misalignment for a breadboard with an amplitude dividing source concept.

- A transversal shift of $0.1\,mm$ of mirror [1] feeding one delay line (see Fig. 8) causes a decentering of the beam, which dramatically degrades the rejection ratio (case 5). By employing a modal filter the rejection ratio is close that of the ideal case (case 3) – of course, only if the optical path delay is adjusted properly.

- The optical path delay is controlled by moving the flat secondary mirror [2] of one delay line. Besides the intended effect of phase shifting there is also the unwanted effect of tilting the output beam, caused by the curvature of the primary mirror. A defocus of $4.1\,\mu m$ causes a tilt of $2\,arcsec$, which, even for ideal optical path delay, degrades the nulling capability (case 6). Due to the tilt, the rejection ratio is dramatically reduced if no filter is used. Even if a modal filter is employed, the rejection ratio is smaller than for the case without misalignment (case 3) because the input beam tilt is transformed by the lens to a lateral shift at the filter's input face.
- A tilt of mirror [3] within the interferometer core by $1\,arcsec$ causes a dramatic reduction of the rejection ratio if no modal filtering is employed (case 7). In case of modal filtering the rejection ratio is somewhat lower than in the case without misalignment (case 3) because of the decentering of the beams at the fibre's input face.

5. CONCLUSION

We clarified the fundamental physical difference between spatial and modal filtering. Spatial filtering means blocking of certain spatial frequencies, while modal filtering means the projection onto a field with predefined amplitude and phase distribution. Thus the spatial filter performance of a pinhole is inferior compared to that of modal filters as the part passing the pinhole is in no way influenced by the spatial filter.

We show that broadband operation of a single modal filter from 4 to 20 microns is not reasonable, not even if we assume an ideal fibre. The reason is dispersion of both coupling efficiency and modefield radius. Within two octaves the coupling efficiency drops to nearly zero, thus dramatically increasing the filter's insertion loss and the modefield radius enlarges drastically, requiring very large cladding diameters.

The exemplary results of a DARWIN-representative nulling interferometer breadboard operating in the near infrared confirm the necessity of modal filtering to attain the required high rejection ratio.

The authors are grateful to A. Frey from Astrium Space GmbH, Germany, for the ray tracing simulations.

REFERENCES

1. A. Léger, J.-M. Mariotti, B. Mennesson, M. Ollivier, J. Puget, D. Rouan, and J. Schneider, "Could we search for primitive life on extrasolar planets in the near future? The DARWIN project," *Icarus* **123**, pp. 373–379, 1997.
2. J. Angel and N. Wolf, "An imaging interferometer to study extrasolar planets," *The Astrophysical Journal* **475**, pp. 373–379, 1997.
3. R. N. Bracewell, "Detecting nonsolar planets by spinning infrared interferometer," *Nature* **274**, pp. 780–782, August 1978.
4. B. Mennesson, M. Ollivier, and C. Ruilier, "Use of single-mode waveguides to correct the optical defects of a nulling interferometer," *Journal of the Optical Society of America* **19**, pp. 596–602, 2002.
5. G. Loos, "Spatial filtering of atmospheric decorrelation from wavefronts for interferometry," *Optics Communications* **99**, pp. 380–392, 1993.
6. M. Ollivier and J.-M. Mariotti, "Improvement in the rejection ratio of a nulling interferometer by spatial filtering," *Applied Optics* **36**(22), pp. 5340–5346, 1997.
7. G. L. Clark and C. Roychoudhuri, "Interferometry through single-mode optical fibers," in *Interferometry, Proc. SPIE 192*, G. W. Hopkins, ed., pp. 196–203, 1979.
8. R. Wagner and W. Tomlinson, "Coupling efficiency of optics in single-mode fiber components," *Applied Optics* **21**(15), pp. 2671–2688, 1982.

9. O. Wallner, W. R. Leeb, and P. J. Winzer, "Minimum length of a single-mode fiber spatial filter," *accepted for publication in the Journal of the Optical Society of America* , 2002.
10. E.-G. Neumann, *Single-Mode Fibers*, vol. 57 of *Springer Series in Optical Sciences*, Springer, 1 ed., 1988.
11. K. Okamoto and T. Okoshi, "Analysis of wave propagation in optical fibers having core with α-profile refractive-index distribution and uniform cladding," *IEEE Transactions on Microwave Theory and Techniques* **24**, pp. 416–421, 1976.
12. T. Birks, J. Knight, and P. Russell, "Endlessly single-mode photonic crystal fiber," *Optics Letters* **22**(13), pp. 961–963, 1997.
13. S. E. Barkou, J. Broeng, and A. Bjarklev, "Silica-air photonic crystal fiber design that permits waveguiding by a true photonic bandgap effect," *Optics Letters* **24**(1), pp. 46–48, 1999.
14. R. Cregan, B. Mangan, J. Knight, T. Birks, P. Russell, P. Roberts, and D. Allan, "Single-mode photonic band gap guidance of light in air," *Science* **285**, pp. 1537–1539, September 1999.
15. E. Marcatili, "Dielectric rectangular waveguide and directional coupler for integrated optics," *Bell System Technical Journal* **48**, pp. 2071–2102, 1969.
16. J. A. Harrington, *Handbook of Optics*, vol. 3, ch. Infrared Fiber Optics. McGraw Hill, 2000.
17. R. Flatscher, U. Johann, and Z. Sodnik, "Nulling breadboard for DARWIN," these proceedings.
18. E. Serabyn and M. M. Colavita, "Fully symmetric nulling beam combiners," *Applied Optics* **40**, pp. 1668–1671, 2001.